JOURNAL OF AGRICULTURAL AND FOOD CHEMISTRY

Article

pubs.acs.org/JAFC

Competitive Interactions of Ionic Surfactants with Salbutamol and Bovine Serum Albumin: A Molecular Spectroscopy Study with Implications for Salbutamol in Food Analysis

Qiulan Zhang,[†,‡] Yongnian Ni,[*,†,‡] and Serge Kokot[§]

[†]State Key Laboratory of Food Science and Technology, Nanchang University, Nanchang 330047, China

[‡]Department of Chemistry, Nanchang University, Nanchang 330031, China

[§]School of Chemistry, Physics and Mechanical Engineering, Science and Engineering Faculty, Queensland University of Technology, Brisbane, Queensland 4001, Australia

Supporting Information

ABSTRACT: The effect of ionic surfactants, sodium dodecyl sulfate (SDS) and *N*-cetyl-*N*,*N*,*N*-trimethylammonium bromide (CTAB), on the interaction between β-agonist salbutamol (SAL) and bovine serum albumin (BSA) was investigated with the use of fluorescence spectroscopy (FLS) and chemometrics methods [multivariate curve resolution-alternating least-squares (MCR-ALS) and parallel factor analysis algorithm (PARAFAC)]. It was found that the binding constant of SAL to BSA in the presence of CTAB was much larger than that without this ligand. The ligand/BSA stoichiometry was 4:1, that is, $(CTAB)_4$−BSA, and was 2:1 with the ligand, that is, $(SAL)_2$−BSA. These results were obtained from the concentration profiles extracted by MCR-ALS for all three reactants. Quantitative information on the complex CTAB−BSA−SAL species was obtained with the resolution of the excitation−emission fluorescence three-way data matrices by PARAFAC. This research has implications for the analysis of SAL in food and might be performed in laboratories associated with organizations such as the U.S. Food and Drug Administration (FDA) and the International Olympic Committee (IOC).

KEYWORDS: *salbutamol, ionic surfactants, bovine serum albumin, fluorescence, BSA−ligand complexes, chemometrics*

INTRODUCTION

The relatively low toxicity and high antimicrobial activity of surfactants make them a particularly valuable means of controlling or preventing microbial growth in the shelf life of food products.[1] However, their actual utilization within the food and beverage industries is rather limited because surfactants tend to accumulate preferentially in lipids and fatty tissue as well as in the liver, kidneys, and serum, in high concentrations and with deleterious results.[2,3] Serum albumin (SA) is the major transport protein in the blood circulatory system (accounting for 52−60% of the total plasma protein);[4] thus, SA plays a major role in the transport and delivery of various endogenous and exogenous compounds, such as metabolites, drugs, and other biologically active substances. Consequently, protein−surfactant interactions have been the subject of extensive studies not only because of their relevance to the above aspects but also because of their importance in many other fields such as foods, pharmaceuticals, paints, and oil extraction among others.[5,6] Commonly, interactions between ionic surfactants and water-soluble proteins have been studied with the use of sodium dodecyl sulfate (SDS)/*N*-cetyl-*N*,*N*,*N*-trimethylammonium bromide (CTAB) and bovine serum albumin (BSA).[7,8]

β_2-Agonists have been used as feed additives for growth promotion in farm animals. The control of chemical residues has become highly questionable to the extent that compulsory residue control regulations have been introduced in China as well as in the European Union (EU).[9] Salbutamol (SAL) is a β_2-selective adrenoreceptor agonist, and such substances produce some anabolic-like effects. Such effects have been observed when these substances are misused as nutrient repartitioning agents in livestock. The role of these substances ranges from diverting nutrients from fat deposition in animals to the production of muscle tissue.[10] Thus, for humans, the International Olympic Committee (IOC) has restricted the use SAL to inhalation only, and the use of such treatment must be declared prior to any competition. In this context, recent research has focused on techniques that perform well in the detection of β_2-selective adrenoreceptor agonists in serum or tissues from treated animals,[11] but only a few studies on the interaction of β_2-selective adrenoreceptor agonist with serum have been published.[12,13]

Conventionally, the pharmacokinetics and pharmacodynamics of a given ligand in the presence of BSA will depend largely on its interaction with this protein; such interactions have been investigated with the use of fluorescence, UV−vis absorption, circular dichroism (CD), and Fourier transform infrared (FT-IR) spectroscopic and electrochemical methods,[14−16] and such measurements have been observed to produce a variety of characteristic parameters including the binding constant, thermodynamic parameters, binding mode, and any effects of the ligand on the stability and conformation of the BSA. Thus, significant information was obtained by these techniques about

Received: March 16, 2013
Revised: July 18, 2013
Accepted: July 22, 2013
Published: July 22, 2013

the nature of this chemical reaction.[17] In general, these data are analyzed individually, and the time dependence of the concentration of a particular compound can be followed by the increase or decrease of the measured signal. However, in many cases, the individual signal bands are not selective because they overlap each other; this precludes further data interpretation by conventional, univariate means. In such cases, which actually occur quite commonly, chemometrics data interpretation methods can overcome most of these problems. In general, in recent years, multidimensional instrumental signals derived from various analytes with the use of modern instrumentation have provided a wide range of quantitative and qualitative results from increasingly complex samples; in this work, such information about the surfactants SAL and BSA was obtained with the resolution of the data matrices by chemometrics methods such as multivariate curve resolution−alternating least-squares (MCR-ALS) and parallel factor analysis algorithm (PARAFAC).

Thus, the aims of this study were (i) to search for and develop spectrofluorometric methods of analysis for the simultaneous determination of ionic surfactants, SDS and CTAB, as well as SAL in their interactions with the BSA protein; (ii) to apply these methods for the collection of spectral data from aqueous solutions containing various combinations of the above reagents at different concentrations and to resolve the expanded matrices of such spectra with the use of chemometrics methods such as MCR-ALS so as to obtain the concentration profiles of the reactants, thereby producing detailed information about the mechanisms of the interactions; and (iii) to resolve the three-way excitation−emission fluorescence spectral matrix, which was obtained from the surfactants, SAL, and BSA solution mixtures, so as to extract the relative concentration profiles of their ternary complexes with the use of the PARAFAC chemometrics method. It was anticipated that the extracted information should provide further mechanistic details on the surfactants, SAL, and BSA interactions, particularly those involving the complicated products of the interactions, which could not be extracted by the MCR-ALS method.

Chemometrics methods have enabled the resolution of multidimensional profiles, which then allow quantitative and qualitative analysis of increasingly complex samples. In this work, qualitative and quantitative information about the surfactants, SAL, and BSA system was obtained with the resolution of the data matrices by chemometrics methods MCR-ALS and PARAFAC.

EXPERIMENTAL PROCEDURES

Apparatus. All fluorescence spectra were measured on a Perkin-Elmer LS-55 spectrofluorometer equipped with a thermostatic bath (model ZC-10, Ningbo Tianheng Instruments Factory, China) with the use of a 1.0 cm quartz cuvette. The excitation and emission slits were set at 10 nm, and the scanning rate was 1200 nm min^{-1}. Titrations were performed manually using suitable micropipets. The FL-WinLab software (Perkin-Elmer) was used to correct the measured data. All of the measurements were carried out at room temperature (25 ± 0.5 °C) unless otherwise stated.

Materials. A stock solution of 5.0×10^{-3} mol L^{-1} salbutamol in sulfuric acid (SAL, Sigma-Aldrich Chemical Co.; purity ≥ 97%) was prepared by dissolving its crystals (0.073 g) in 50 mL of distilled water. To confirm the purity of the prepared BSA (2×10^{-3} mol L^{-1}), the concentration was diluted to 1.47×10^{-5} mol L^{-1}, and the measured absorbance value was 0.660 at 278 nm. This compared well with the expected reference absorbance value of 0.667 at 278 nm for 1.0 g L^{-1} (1.47×10^{-5} mol L^{-1}) pure BSA.[18] Warfarin (Medicine Co. Ltd., Shanghai, China) and ibuprofen (Baike Hengdi Pharmaceutical Co. Ltd., Hubei, China) stock solutions (2.5×10^{-3} mol L^{-1}) were prepared by dissolving weight aliquots of each compound in water. Sodium dodecyl sulfate (SDS) and *N*-cetyl-*N*,*N*,*N*-trimethylammonium bromide (CTAB; Medicine Co. Ltd.) solutions of 5.0×10^{-3} mol L^{-1} were prepared by dissolving their crystals (0.072 and 0.092 g) in 50 mL of distilled water, respectively. Other chemicals were analytical grade reagents, and doubly distilled water was used throughout. All experimental solutions were adjusted with the Tris-HCl ((hydroxymethyl)aminomethane−hydrogen chloride) buffer (ca. 3.0 mL) to pH 7.4, and the added volume of analytes (BSA and SAL or surfactant) was generally <0.1 mL.

Experimental Details of the Interactions Involving the Binary Systems SAL/CTAB/SDS−BSA. *Experiment 1.* The concentration of BSA (1.33×10^{-7} mol L^{-1}) was kept constant throughout, and SAL was added to this solution in the range of $(0.00-2.13) \times 10^{-7}$ mol L^{-1} (in steps of 2.67×10^{-8} mol L^{-1}). These well-mixed solutions were allowed to stand for 10 min at 298, 301, and 304 K before spectroscopic measurements.

Experiment 2. The concentration of BSA was kept constant (1.33×10^{-7} mol L^{-1}), and CTAB or SDS was added to the BSA solution in the range of $(0.00-4.26) \times 10^{-7}$ mol L^{-1} (in steps of 5.33×10^{-8} mol L^{-1}) at 298 K.

Experiment 3. The concentration of BSA was kept constant (1.33×10^{-7} mol L^{-1}), and SDS was added to the solution in the range of $(0.00-1.07) \times 10^{-6}$ mol L^{-1} (in steps of 5.33×10^{-8} mol L^{-1}). Fluorescence spectra were then measured in the range of 300−500 nm at the excitation wavelength of 280 nm.

Development of the Expanded Data Matrix. The mole ratio method was used for the following four experiments.

Experiment 1. The concentration of BSA was kept constant (6.67×10^{-8} mol L^{-1}), and SAL was added to the solution in the range of $(0.00-2.67) \times 10^{-7}$ mol L^{-1} (in steps of 1.33×10^{-8} mol L^{-1}).

Experiment 2. The concentration of SAL was kept constant (6.67×10^{-8} mol L^{-1}), and BSA was added to the solution in the range of $(0.00-6.67) \times 10^{-8}$ mol L^{-1} (in steps of 3.33×10^{-9} mol L^{-1}).

Experiment 3. The concentration of BSA was kept constant (1.33×10^{-7} mol L^{-1}), and CTAB was added to the solution in the range of $(0.00-1.07) \times 10^{-6}$ mol L^{-1} (in steps of 5.33×10^{-8} mol L^{-1}).

Experiment 4. The concentration of CTAB was kept constant (1.33×10^{-7} mol L^{-1}), and BSA was added to the solution in the range of $(0.00-6.67) \times 10^{-8}$ mol L^{-1} (in steps of 3.33×10^{-9} mol L^{-1}).

The fluorescence output (300−500 nm) of the above four experiments was recorded every 0.5 nm. Thus, two sets of data matrices D_F^{BSA} and D_F^{SAL} (experiments 1 and 2) and D_F^{BSA} and D_F^{CTAB} (experiments 3 and 4) were obtained. The two different column-wise spectral data matrices were combined, and two expanded data matrices, $\begin{bmatrix} D_F^{BSA} \\ D_F^{SAL} \end{bmatrix}$ and $\begin{bmatrix} D_F^{BSA} \\ D_F^{CTAB} \end{bmatrix}$, were thus obtained. They were subsequently resolved by the MCR-ALS method.

Fluorescence Spectra in the Presence of the Site Markers. To identify the binding sites of SAL and SDS or CTAB on BSA, warfarin and ibuprofen were used as the markers for sites I and II, respectively. The ratios of warfarin/BSA and ibuprofen/BSA were all kept at 1:1 (both 6.67×10^{-8} mol L^{-1}), respectively, and then SAL [$(0.00-2.13) \times 10^{-7}$ mol L^{-1}, in steps of 2.67×10^{-8} mol L^{-1}] or CTAB (SDS) [$(0.00-4.26) \times 10^{-7}$ mol L^{-1}, in steps of 5.33×10^{-8} mol L^{-1}] was added. In all cases, fluorescence spectra were measured as previously described. The binding constants, K_a, of SAL, CTAB, and SDS were then estimated from the results of these experiments.

Experimental Details for the Interactions Involving Ternary Systems ($CTAB_4$−BSA)−SAL and (SDS_3−BSA)−SAL. *Experiment 1.* The molar ratio of CTAB/BSA was kept at 4:1 (CTAB and BSA were 2.67×10^{-7} and 6.67×10^{-8} mol L^{-1}, respectively), and SAL was added to this solution in the range of $(0.00-2.67) \times 10^{-7}$ mol L^{-1} in steps of 1.33×10^{-8} mol L^{-1}.

Experiment 2. The ratio of SDS/BSA was kept at 3:1 (SDS and BSA were 4.00×10^{-7} and 1.33×10^{-7} mol L^{-1}, respectively), and

dx.doi.org/10.1021/jf402316j | J. Agric. Food Chem. 2013, 61, 7730−7738

SAL was added to this solution in the range of $(0.00-2.13) \times 10^{-7}$ mol L^{-1} in steps of 2.67×10^{-8} mol L^{-1}.

Experiment 3. The ratio of SDS/BSA was kept at 3:1 (SDS and BSA were 4.00×10^{-7} and 1.33×10^{-7} mol L^{-1}, respectively), and SAL was added to this solution in the range of $(0.00-1.07) \times 10^{-6}$ mol L^{-1} in steps of 1.33×10^{-7} mol L^{-1}.

Experimental Details for the Competitive Reaction of CTAB and SAL with BSA. Four microliters of BSA (5.0×10^{-5} mol L^{-1}), 40.0 μL of CTAB (2.0×10^{-5} mol L^{-1}), and 3.0 mL of Tris-HCl buffer (pH 7.4) were transferred to a 10 mm quartz cuvette. SAL was added to the solution at different concentrations in the range of $(0-2.00) \times 10^{-7}$ mol L^{-1} in steps of 1.33×10^{-8} mol L^{-1} to give a series of 16 samples. All samples were measured in the excitation range of 230–350 nm (every 5 nm) and in the emission range of 300–450 nm (every 0.5 nm). Thus, the obtained three-way excitation–emission fluorescence matrix (EEM) data had the dimensions of 21 (samples) × 25 (λ_{em}) × 301 (λ_{ex}) as defined by the $I \times J \times K$ dimensions for system of $(CTAB_4-BSA)-SAL_2$ complex.

CHEMOMETRICS METHODS

Multivariate Curve Resolution–Alternating Least Squares (MCR-ALS). The obtained data matrices were resolved by the MCR-ALS method, which is a multivariate, self-modeling curve resolution procedure developed by Tauler.[19] It involves a bilinear decomposition of an experimental data set, $\boldsymbol{D}$, to obtain matrices, $\boldsymbol{C}$ and $\boldsymbol{S}^{\mathrm{T}}$, which have a real chemical significance, according to equation 1

$$\boldsymbol{D} = \boldsymbol{C}\boldsymbol{S}^{\mathrm{T}} + \boldsymbol{E} \tag{1}$$

where $\boldsymbol{D}$ is the experimental data matrix with dimensions M (spectral objects) × N (wavelengths); $\boldsymbol{C}$ $(M \times F)$ is the concentration profile matrix from F analytes in the samples; $\boldsymbol{S}^{\mathrm{T}}(F \times N)$ is the transposed matrix of emission spectra, the F rows of which contain the pure spectra associated with the F species in the samples; and $\boldsymbol{E}(M \times N)$ is the residuals matrix. The experimental spectral data matrix, $\boldsymbol{D}$, is resolved as follows:[20]

When two different chemical systems are monitored using a fluorescence technique, a column-wise enlarged data matrix can be built up. The individual data matrices corresponding to the two types of spectra are combined. The related bilinear model for MCR-ALS analysis is given by eq 2:

$$\begin{bmatrix} D_{\mathrm{F}}^{\mathrm{BSA}} \\ D_{\mathrm{F}}^{\mathrm{ligand}} \end{bmatrix} = \begin{bmatrix} \boldsymbol{C}^{\mathrm{BSA}} \\ \boldsymbol{C}^{\mathrm{ligand}} \end{bmatrix} [\boldsymbol{S}_{\mathrm{F}}^{\mathrm{T}}] + \boldsymbol{E}_{\mathrm{F}} \tag{2}$$

If $D_{\mathrm{F}}^{\mathrm{BSA}}$ and $D_{\mathrm{F}}^{\mathrm{ligand}}$ are the measurements from the two experiments obtained with the fluorescence spectra, there are two concentration profile matrices, $\boldsymbol{C}^{\mathrm{BSA}}$and $\boldsymbol{C}^{\mathrm{ligand}}$, that contain the two sets of raw measurements and a column-wise enlarged spectral matrix where $\boldsymbol{S}_{\mathrm{F}}^{\mathrm{T}}$ contains the pure spectra for the technique used to obtain $D_{\mathrm{F}}^{\mathrm{BSA}}$ and $D_{\mathrm{F}}^{\mathrm{ligand}}$, respectively. Solving eq 2 for $\boldsymbol{C}^{\mathrm{BSA}}$, $\boldsymbol{C}^{\mathrm{ligand}}$, and $\boldsymbol{S}_{\mathrm{F}}^{T}$ facilitates the extraction of the related spectral objects of all the species in the system.[21]

When the matrix $\begin{bmatrix} D_{\mathrm{F}}^{\mathrm{BSA}} \\ D_{\mathrm{F}}^{\mathrm{ligand}} \end{bmatrix}$ of the two data matrices is being built, the number of analytes, F, can be obtained with the aid of evolving factor analysis (EFA)[22] or principal component analysis (PCA). EFA provides an estimation of the regions or windows where the concentration of different components is changing or evolving; it also provides an initial estimation of how these concentration profiles change during the experiment. The EFA method is based on the evaluation of the magnitude of the eigenvalues associated with all of the submatrices of a matrix built by adding successively all of the rows of the original data matrix. The calculation is performed in two directions: forward (in the same direction of the experiment) and backward (in the opposite direction of the experiment). The concentration profiles from EFA were used as the initial estimate for the concentration matrix input in the constrained ALS optimization.[23]

PCA is a common data display method, which transforms the original data into the same number of orthogonal variables (principal components, PCs) but usually only a few PCs are required to account for the significant information in the data matrix. Thus, the original data are usually compressed to fewer PCs than the number of original variables, and each object is associated with a score value and each PC with a loadings value. PC-by-PC plots of objects and variables provide information regarding the object–object, variable–variable, and object–variable associations.[24]

The iterative ALS procedure requires initial values for the spectral or concentration profiles for each species;[20] these can be obtained with the application of SIMPLISMA[25] and an EFA plot, respectively. In this work, such initial estimates were made with the use of the "most pure concentrations" method.[26]

This kind of simultaneous data analysis is more powerful compared to that described by eq 1 and allows for improved resolution of complex data structures.[21,27] In general, the method produces more reliable solutions because it eventually removes rotational ambiguities and rank-deficiency problems as described in the literature.[20]

Parallel Factor Analysis Algorithm. According to the work of Leurgans and Ross,[28] fluorescence spectroscopy can be described by means of multiway approaches. To extract the information from the EEM, the PARAFAC method may be applied.[29,30] This method is a generalization of bilinear PCA to higher order arrays. In other words, PARAFAC decomposes N-way arrays into N loading matrices. Unlike PCA, a PARAFAC model provides unique solutions and there are no additional orthogonality constraints. This means that if the underlying structure of the three-way data coincides with the PARAFAC model, then the parameters of the PARAFAC model will reflect the true underlying parameters. Hence, in the context of fluorescence spectroscopy, each fluorophore will give rise to one PARAFAC component,[31] and the scores of components indicate the relative concentrations of the different fluorophores. An important advantage of the multiway methods over the data unfolding ones is that the estimated models for the former are mathematically quite simple and, therefore, more robust and easier to interpret.[32] An EEM contains all of the steady state fluorescence features of a fluorophore as well as the fluorescence intensity at particular excitation and emission wavelengths. If fluorescence EEMs are arranged in a three-way array, $\boldsymbol{X}$, of dimensions $I \times J \times K$, where I is the number of samples, J is the number of excitation wavelengths, and K is the number of emission wavelengths, PARAFAC decomposes $\boldsymbol{X}$ into three matrices. These are labeled $\boldsymbol{A}$ (the score matrix) and $\boldsymbol{B}$ and $\mathbf{C}$ (the loading matrices) with elements a_{if}, b_{jf}, and c_{kf}, respectively. Let X_{ijk} denote the element in position i, j, and k in matrix $\boldsymbol{X}$, and then the structural model of PARAFAC may be expressed as

$$X_{ijk} = \sum_{f=1}^{F} a_{if} b_{jf} c_{kf} + e_{ijk} \tag{3}$$

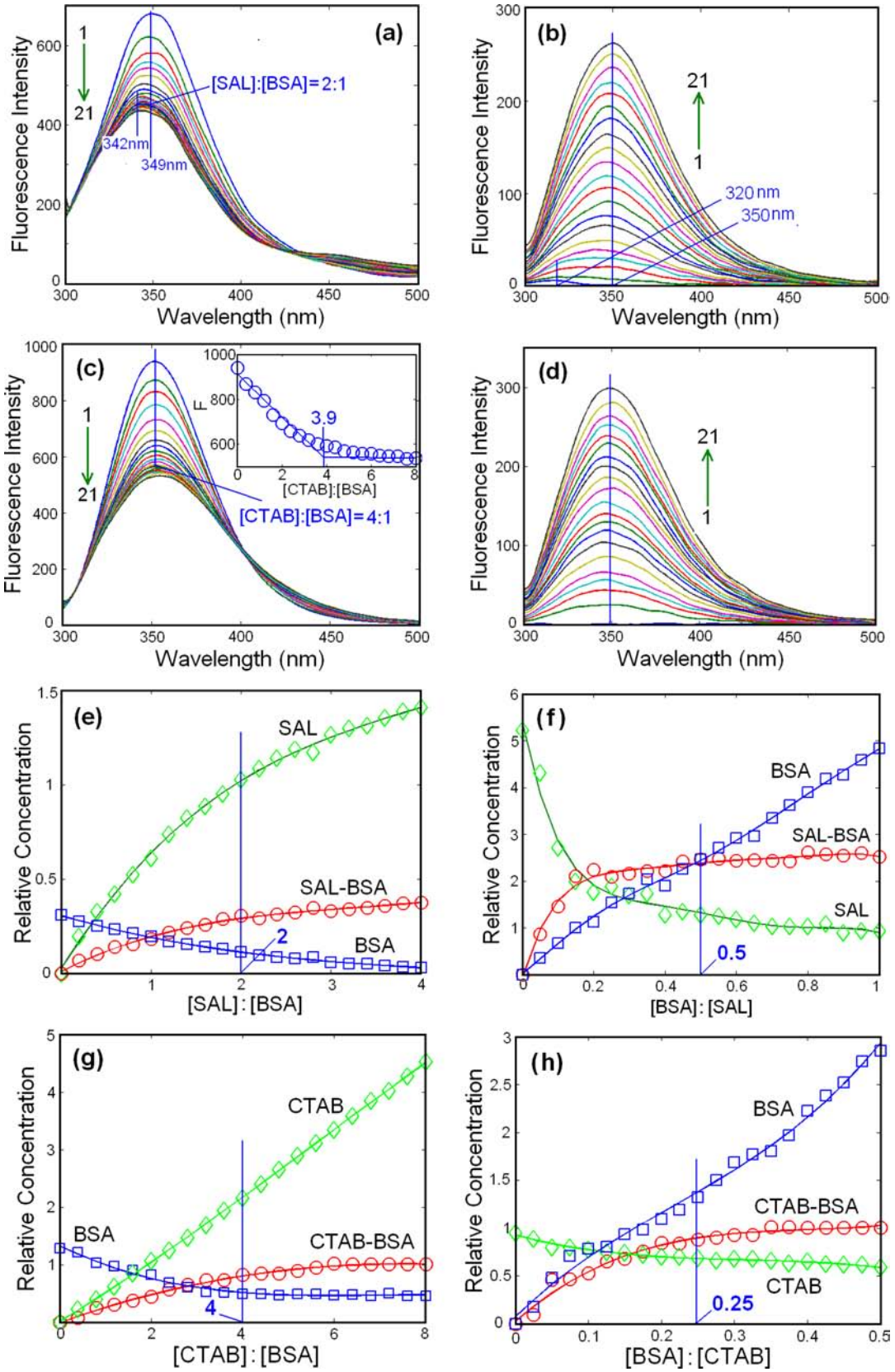

Figure 1. Fluorescence spectra obtained from different experiments: experiment 1 and 2 [(a) (D_F^{BSA}) and (b) (D_F^{SAL}] and experiments 3 and 4 [(c) (D_F^{BSA}) and (d) (D_F^{CTAB}]. Concentration profiles recovered by the MCR-ALS method: (e) and (f) for experiments 1 and 2; (g) and (h) for experiments 3 and 4.

$(i = 1, \ldots, I;\ j = 1, \ldots, J;\ k = 1, \ldots, K)$

where F is the number of factors, that is, the analytes present in the sample, a_{if}, b_{jf}, and c_{kf} are the elements of the three loading

dx.doi.org/10.1021/jf402316j | J. Agric. Food Chem. 2013, 61, 7730−7738

vectors $\boldsymbol{a}_f$, $\boldsymbol{b}_f$, and $\boldsymbol{c}_f$, and e_{ijk} denotes the residual error. If the experimental data are trilinear and there are F fluorescent components in the samples, the model of F components can be used to estimate (i) the extinction coefficients for each analyte, f, at all wavelengths, that is, the excitation profile, $\boldsymbol{b}_f = (b_{1f}, b_{2f}, ..., b_{Jf})$, or excitation spectrum; (ii) the relative emission at all wavelengths, that is, the emission profile, $\boldsymbol{c}_f = (c_{1f}, c_{2f}, ..., c_{kf})$, or the emission spectrum of each analyte; and (iii) the relative concentration of every analyte in all samples, that is, the sample profile, $\boldsymbol{a}_f = (a_{1f}, a_{2f}, ..., a_{If})$. Vectors $\boldsymbol{b}_f$ and $\boldsymbol{c}_f$ are usually normalized to unit length.

When experimental data correspond to eq 3, that is, data are trilinear, the PARAFAC decomposition method[33] provides unique profile estimations. This means that, provided the rank of the PARAFAC model corresponding to the number of fluorescence compounds, each with a PARAFAC factor, f, can be assigned to a compound and the loadings (a_{if}, b_{jf}, and c_{kf}) can be interpreted as an estimation of the relative analyte concentrations, excitation spectra, and emission spectra, respectively. Andersen and Bro[34] presented a detailed investigation and practical description of how to apply PARAFAC modeling to fluorescence excitation−emission measurements, and a review of recent chemical applications of PARAFAC is provided elsewhere.[35]

RESULTS AND DISCUSSION

Fluorescence Quenching Mechanism of BSA in the Presence of SAL. Different quenching mechanisms are usually classified as either dynamic or static, and these can be distinguished by their different dependence on temperature and viscosity.[36] The role of fluorescence quenching can be studied experimentally by determining the quenching rate parameters using Stern−Volmer plots.[37] In this work, the intrinsic fluorescence spectrum of BSA was strongly quenched on addition of the SAL ligand at different temperatures (Experiment 1, under Experimantal Details for Interactions Involving the Binary Systems SAL/CTAB/SDS−BSA), and to establish the fluorescence quenching mechanism, the fluorescence spectral data for BSA were analyzed with the use of the Stern−Volmer equation

$$F_0/F = 1 + K_{SV}[Q] \quad (4)$$

where F_0 and F represent the fluorescence intensities in the absence and presence of the quencher, respectively. K_{SV} is the Stern−Volmer dynamic quenching constant, and [Q] is the concentration of quencher. The fluorescence quenching data of BSA in the presence of different complexes at three temperatures of 298, 301, and 304 K were processed by eq 4, respectively. The calculated K_{SV} at each temperature (2.03×10^6, 1.39×10^6, and 1.07×10^6 L mol^{-1}) showed that the Stern−Volmer quenching constant, K_{SV}, is inversely correlated with temperature, and this indicated that the probable quenching mechanism of the SAL−BSA binding reaction is initiated by the SAL−BSA complex formation rather than by a dynamic collision.[38]

Ligand−BSA Equilibrium. Fluorescence quenching data from the interaction of ligands with BSA were analyzed to obtain various binding parameters (Experiments 1−3 under Experimantal Details for the Interactions Involving the Binary Systems SAL/CTAB/SDS−BSA). The binding constant (K_b) and binding number (n) were calculated from the equation[39]

$$\log[(F_0 - F)/F] = \log K_b + n \log[Q] \quad (5)$$

The order of magnitude of K_b of 10^6 L mol^{-1} illustrated that there was a strong binding force between SAL and BSA. The values of K_b (3.12×10^6, 2.22×10^6, and 1.89×10^6 L mol^{-1}) indicated that there was a strong binding force between SAL and BSA, and the decrease of the association constants with increasing temperature (298, 301, and 304 K) suggested that the SAL−BSA complex was progressively destabilized. Additionally, the values of n were approximately 1, which indicated that there was just one binding site for SAL in the BSA protein. According to eq 5, the values of n for CTAB and SDS were 0.837 and 0.978, that is, approximately 1, which indicated that there was just a single binding site in BSA for either CTAB or SDS.

Resolution of Ligand Binding to BSA with the Use of MCR-ALS. Tryptophan fluorescence is commonly used to monitor changes in protein structure and to explore the associated local structure and dynamics.[40] Thus, fluorescence data (Experiments 1−4 under Development of the Expanded Data Matrix) obtained from the interaction between either SAL or CTAB and BSA were used to build the expanded matrices previously discussed. Thus, two such matrices, $\begin{bmatrix} D_F^{BSA} \\ D_F^{SAL} \end{bmatrix}$ and $\begin{bmatrix} D_F^{BSA} \\ D_F^{CTAB} \end{bmatrix}$ corresponding to Figure 1a,b and Figure 1c,d were obtained and resolved with the use of the MCR-ALS method, respectively. The emission spectra of BSA in the presence of different concentrations of SAL (Figure 1a) indicated that the fluorescence intensity of BSA at 350 nm decreased systematically with increasing SAL concentration, but when the ratio, $r_{SAL\text{-}BSA}$, reached 2:1, the spectral intensity flattened out and a small blue shift (ca. 7 nm) was observed. These observations could be reflecting small conformational changes of tryptophan and tyrosine microstructure resulting from the interaction of SAL with BSA in the secondary structure of the protein.[18] The fluorescence emission spectra of SAL in the presence of BSA at different concentrations showed (Figure 1b) that on titration with BSA, the emission spectrum of SAL (curve 1) at 320 nm was subsumed by the gradually forming, more intense, new band at 350 nm (curve 3); it was assigned to the added BSA. In contrast, the fluorescence spectra obtained from the CTAB−BSA interaction (Figure 1c,d) provided rather less information. Thus, the fluorescence intensity decreased slowly (Figure 1c), but when the ratio of $r_{CTAB\text{-}BSA}$ almost reached 4 (inset, Figure 1c, intersection of the two straight lines), the peak intensity flattened out on further increase of the CTAB concentration. This is consistent with the CTAB−BSA interaction reaching an equilibrium; no further significant information could be obtained from Figure 1d, except that the peak intensity continued to increase steadily.

Generally, from the individual fluorescence spectra above (Figure 1a−d), it was difficult to deduce the formation of a complex in the binding reaction system because of the significant spectral overlap of the various species. Also, although MCR-ALS is a powerful chemometric tool, it is possible that the analysis of the individual data sets by this method may encounter unresolved underlying factor analysis ambiguities,[19] which could complicate the interpretation of results. Therefore, in this work, the data matrices were combined into two column-wise expanded data matrices, $\begin{bmatrix} D_F^{BSA} \\ D_F^{SAL} \end{bmatrix}$ and $\begin{bmatrix} D_F^{BSA} \\ D_F^{CTAB} \end{bmatrix}$, respectively, as previously explained, and these were submitted for simultaneous resolution by the MCR-ALS method. The

intention here was to obtain information regarding the ligand–BSA complexes, the concentration of the profiles of the various reacting species, and any effects of the ligands on the protein's substructure. Thus, after the construction of the expanded data matrix, the number of factors, that is, the chemical species, were estimated with the use of the EFA procedure, which is based on an examination of the wavelength evolution of the rank of matrix, ***D***, in forward and back directions. The results indicated that there were three significant factors that accounted for the significant data variance of the two data matrices. PCA was also employed to select the appropriate number of components to describe the two systems with similar results. The three major components explained 99.78 and 99.82% of the total variance of the two data matrices, $\begin{bmatrix} D_F^{BSA} \\ D_F^{SAL} \end{bmatrix}$ and $\begin{bmatrix} D_F^{BSA} \\ D_F^{CTAB} \end{bmatrix}$, respectively.[41] Thus, the EFA and PCA methods estimated the same number of factors or chemical species involved. These three factors were postulated to be free BSA, free SAL or CTAB, and the ligand–BSA complex.[20] The MCR-ALS method was then applied with the use of the initial estimate of the concentration profiles, which were obtained from the EFA for the three postulated species. The concentration calculations were optimized with the modeling constraints: (i) the results were to be positive or zero and (ii) unimodel profiles were to be extracted. Also, as the total concentrations of the ligand and BSA were known in the experiments, they were included as a closure constraint for the concentration profiles.

The concentration profiles recovered by the MCR-ALS method (Figure 1e–h) from the results of the mole–ratio experiment with constant values of the c_{BSA} and c_{ligand} (Experiments 1–4 under Development of the Expanded Data Matrix) showed that (i) for SAL, with the mole–ratio method, the concentration of the intercalation complex increased sharply and reached an equilibrium when $r_{SAL\text{-}BSA} \sim 2$ (Figure 1e,f) and (ii) for CTAB, the concentration of the intercalation complex increased slowly to $r_{CTAB\text{-}BSA} \sim 4$ and approached the equilibrium position as the concentration of CTAB increased (Figure 1g,h). Thus, from these results it would appear that for the SAL–BSA interaction, the equilibrium position suggested a $(SAL)_2$–BSA complex formation, whereas for the CTAB–BSA complex the ratio was 4 and a $CTAB_4$–BSA complex was obtained (Figure 2a,b; two molecules of salbutamol (SAL) combined with one of BSA and four molecules of CTAB combined with one of BSA).

The emission spectra of BSA in the presence of different concentrations of SDS (Figure 3) were also measured (Experiment 3 under Experimental Details for Interactions Involving the Binary Systems SAL/CTAB/SDS–BSA), and they indicated that the fluorescence intensity of BSA at 350 nm decreased systematically with increasing SDS concentration, but when the ratio, $r_{SDS\text{-}BSA}$, reached 3:1, the fluorescence intensity flattened out, which indicated the formation of an $(SDS)_3$–BSA complex, and a small blue shift was observed. Elsewhere, Kelley and McClements[42] found that three SDS molecules bound to the high-affinity site of BSA through a combination of electrostatic and hydrophobic interactions; they also suggested that the ratio of the SDS–BSA complex was 3:1 (Figure 2c, three molecules of SDS combined with one of BSA).

Effect of Warfarin and Ibuprofen Site Markers on the Binding of the Ligands to BSA. The crystal structure of BSA shows that it is a heart-shaped helical monomer composed of

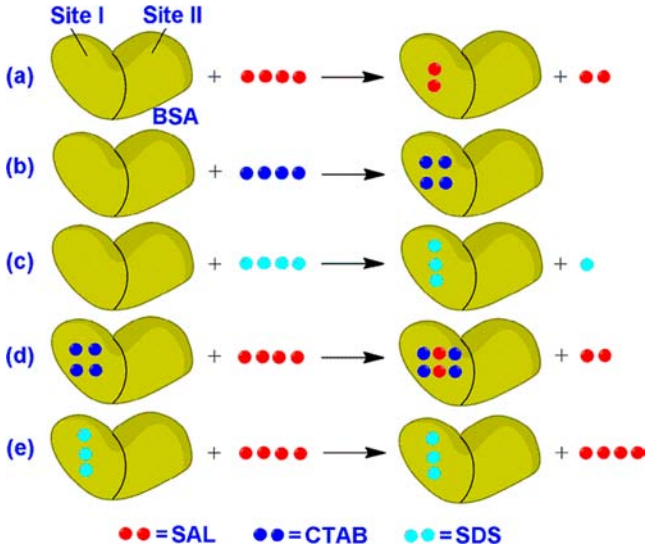

Figure 2. Competitive binding of SAL, CTAB, and SDS to BSA. In particular, note (d) SAL and CTAB bind together in the cavity of site I and (e) SAL binds to the outer site I, whereas SDS is stabilized inside the cavity of this site.

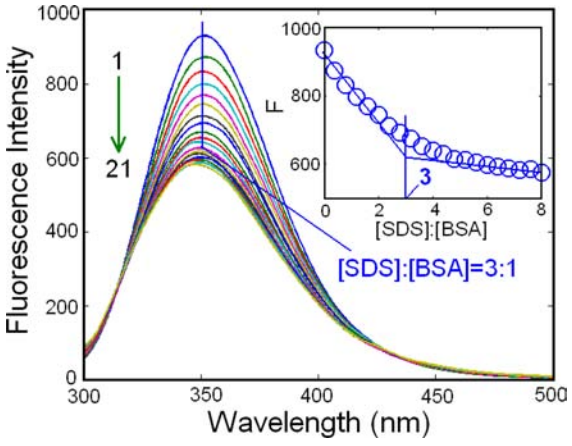

Figure 3. Fluorescence emission spectra of the binary complex SDS–BSA. Concentrations: $C_{BSA} = 1.33 \times 10^{-7}$ mol L^{-1} and $C_{SDS} = (0.00–1.07) \times 10^{-6}$ mol L^{-1} (in steps of 5.33×10^{-8} mol L^{-1}).

three homologous domains, I, II, and III, each of which includes two subdomains, A and B. The principal regions of ligand binding sites on the serum albumin are found in hydrophobic cavities in subdomains IIA and IIIA; these locations have similar chemical properties[43] and are referred to as sites I and II.[44] In general, marker molecules specific to a site are used to establish the particular binding site of a ligand such as CTAB, SDS, and SAL, by competitive reactions. From X-ray crystallography studies, warfarin has been demonstrated to bind to subdomain IIA, whereas ibuprofen binds to subdomain IIIA.[45] Thus, information about the ligand binding site can be obtained by monitoring the changes in the fluorescence of a ligand bound to serum albumin either at site I (warfarin) or at site II (ibuprofen) marker.

In this work, during a site marker competitive experiment, SAL, CTAB, and SDS were gradually added to a solution containing equimolar amounts of BSA and the two above site markers (6.67×10^{-8} mol L^{-1}). To facilitate a comparison of the influence of warfarin and ibuprofen site markers on the

dx.doi.org/10.1021/jf402316j | J. Agric. Food Chem. 2013, 61, 7730–7738

binding of SAL, CTAB, and SDS to BSA, the spectral fluorescence quenching data of the ligand−BSA system in the presence of the site markers were processed with the use of eq 5. The results of such experiments (Fluorescence Spectra in the Presence of the Site Markers) indicated that the binding constants of the systems with warfarin were almost 30, 40, and 50% of those without warfarin for SAL, CTAB, and SDS, respectively; on the other hand, the constants of the systems with and without ibuprofen had only small differences. This indicated that warfarin was significantly affected by the competing ligands, SAL, CTAB, and SDS, to BSA, and ibuprofen had only a small influence. These observations indicated that the SAL, CTAB, and SDS ligands were mainly located within site I (subdomain IIA)[46] in the BSA protein.

Multiple Ligand−BSA Interactions: Ternary System. The large hydrophobic cavity in the BSA protein can accommodate two or more ligands, and in the binding process, two types of interaction can occur:[47] (i) competitive binding, that is, one ligand effectively is preferred to another; and (ii) noncompetitive binding, that is, each ligand binds independently of any other.

Thus, a series of experiments were carried out as indicated under Experimental Details for Interactions Involving the Ternary Systems ($CTAB_4$−BSA)−SAL and (SDS_3−BSA)−SAL. When SAL was added to the $CTAB_4$−BSA mixture, the fluorescence band of the $CTAB_4$−BSA complex at 350 nm gradually decreased in intensity (Figure 4). Because the CTAB

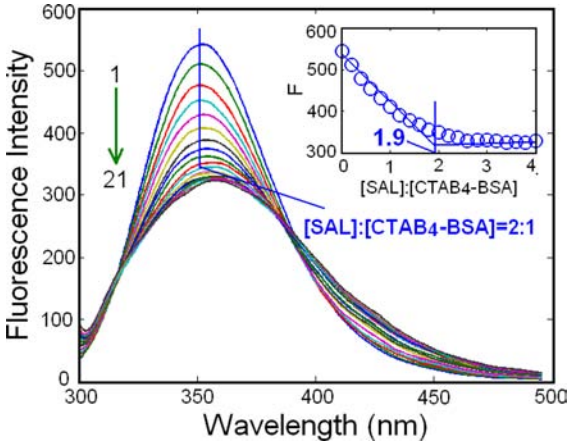

Figure 4. Fluorescence emission spectra of the binary complex $CTAB_4$−BSA, titrated with SAL. Concentrations: BSA and CTAB, 6.67×10^{-8} and 2.67×10^{-7} mol L^{-1}, respectively; C_{SAL}, added in the range of $(0.00–2.67) \times 10^{-7}$ mol L^{-1} in steps of 1.33×10^{-8} mol L^{-1}.

does not fluorescence, it is difficult to estimate whether the CTAB ligand was displaced by SAL. The fluorescence intensity appeared to have leveled off when the ratio of [$CTAB_4$−BSA]/[SAL] was nearly equal to 1:2 (inset, Figure 4, note the intersection of two straight lines). However, it was shown that the binding constant SAL to BSA in the case of the ternary system with CTAB, ($K_a = 9.56 \times 10^6$ L mol^{-1}), was much larger than the binary system without CTAB, ($K_a = 3.12 \times 10^6$ L mol^{-1}). This suggested that the binding force between the protein and one of the β_2-selective adrenoreceptor agonists increased in the presence of the cationic surfactant, CTAB, and this is consistent with the deprotonation of the SAL ligand to form a negative ion:

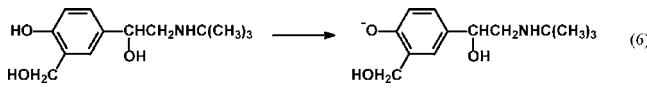

(6)

Thus, CTAB was attracted to the anionic SAL (Figure 2d, SAL and CTAB bind together in the cavity of site I), which was reflected in the rise of the value of the binding constant between SAL and BSA. However, when SAL was added to the SDS_3−BSA mixture, the fluorescence intensity at 350 nm decreased much less than that noted for the [$CTAB_4$−BSA]/[SAL] case (Figure 4). When the concentration of SAL was increased 5-fold in the SDS_3−BSA mixture, the fluorescence intensity at 350 nm decreased much less as well (Experiments 2 and 3 under Experimental Details for Interactions Involving the Ternary Systems ($CTAB_4$−BSA)−SAL and (SDS_3−BSA)−SAL). Thus, the fluorescence intensity of BSA at 350 nm decreased differently in the presence or absence of the ionic surfactant SDS. When SAL was added to the SDS_3−BSA mixture, the dissociated SAL anion and the anionic surfactant SDS repulsed each other, which prevented the SAL molecule from approaching the Trp residue of BSA (Figure 2e, SAL binds to the outer site I, whereas SDS is stabilized inside the cavity of this site).

The above interpretation of SAL binding with BSA (Figure 2d,e) provides an interesting rationalization, which could be of significance for the testing of the SAL compound in foods by, for example, any laboratories associated with FDA and IOC. Furthermore, in the presence of surfactants, such as CTAB, the binding of SAL with BSA will become much stronger and the metabolism of SAL will be reduced or even prevented; hence, the detection of SAL in meat should become easier in such cases; on the other hand, in the presence of SDS, the trend of the interaction of BSA with SAL should be significantly reduced, and this should facilitate the metabolism of SAL but hinder the analysis of SAL in meat.

Decomposition of the Three-Way Fluorescence EEM Data by PARAFAC. The ternary SAL, CTAB, and BSA complex systems were investigated further so as to elucidate their nature and the complex interactions. The binary $CTAB_4$−BSA solutions were prepared, and then an aliquot of the SAL β-agonist was added to these samples (Experimental Details for the Competitive Reaction of CTAB and SAL with BSA). Fluorescence spectra were measured for a set of such solutions, and thus a three-way data array was obtained with the dimensions of 21 × 25 × 301 for ($CTAB_4$−BSA)−SAL_2 together with the spectral intensities at 301 wavenumbers. A three-factor PARAFAC model was chosen to resolve each of the two systems with overlapping spectral profiles that led to the concentration profiles for the three interacting species, SAL, $CTAB_4$−BSA, and ($CTAB_4$−BSA)−SAL. In general, for EEM analysis, Rayleigh scattering contribution should be eliminated prior to multilinear decomposition. Methods for doing this are discussed in detail elsewhere.[32] In this work, the Rayleigh scattering response, measured with a buffer solution, was subtracted from the spectra of the analyzed mixtures to minimize this effect.

The concentration loadings (a_f in eq 3, $f = 1–3$) of a three-component PARAFAC solution for the three-way data array (Figure 5) showed that the concentration of the complex, $CTAB_4$−BSA, decreased and that of the ternary complex, $CTAB_4$−BSA−SAL_2, increased gradually with increasing concentration of the added SAL. The plot flattened out and reached a concentration equilibrium when the ratio of [SAL]/

dx.doi.org/10.1021/jf402316j | J. Agric. Food Chem. 2013, 61, 7730−7738

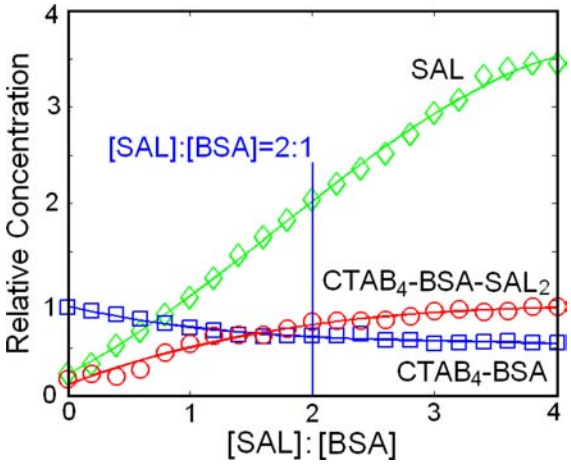

Figure 5. Relative concentrations of the complexes $CTAB_4$–BSA, $CTAB_4$–BSA–SAL_2, and SAL as extracted by PARAFAC and plotted against SAL concentrations.

[BSA] was about 2.0. Given that the initial concentration of the $CTAB_4$–BSA was kept constant, the concentration of the complex $CTAB_4$–BSA–SAL_2 was consistent with the proposition that the SAL interacted with the $CTAB_4$–BSA, presumably through the formation of a ternary complex, ($CTAB_4$–BSA)–SAL_2 (Figure 2d). This strengthened the interaction between the cationic surfactant and SAL with BSA. The formation of the ternary complex could be followed clearly (Figure 5), and the results indicated that both CTAB and SAL bonded in site I of the BSA simultaneously; that is, there was cooperative rather than competitive binding of the two ligands to the protein.

In conclusion, simultaneous methods of analysis for the complex ligand–protein species formed during the interactions of the ionic surfactant, salbutamol, and BSA were researched and developed with the use of fluorescence spectroscopy and chemometrics methods, MCR-ALS and PARAFAC. Resolution of the excitation–emission fluorescence three-way data with the use of these methods provided otherwise inaccessible information. Thus, the concentration profiles of each species at equilibrium were extracted, and this facilitated the interpretation of the mechanism of the interaction between the surfactants, SAL and BSA.

Specific findings included the following: Stern–Volmer quenching constant values indicated a static quenching mechanism in the interactions of SAL with BSA. Associated information suggested only one high-affinity binding site in BSA for SAL or CTAB/SDS ligands; spectrofluorometric data matrices were simultaneously analyzed (MCR-ALS) and the extracted concentration profiles indicated that 2:1 SAL_2–BSA and 4:1 $CTAB_4$–BSA fluorescent binary complexes were formed at equilibrium; quenching fluorescence studies (PARAFAC) revealed the formation of a ternary complex, $CTAB_4$–BSA–SAL_2; its formation suggested an increased affinity for SAL; that is, it is difficult for SAL to metabolize, and SAL is more likely to be detected in foodstuffs of animal origin. However, in the case of the SDS_3–BSA complex mixture, SAL is more exposed; that is, it is more easily metabolized, and it is more difficult to detect in foodstuff of animal origin.

MCR-ALS and PARAFAC can be successfully applied to data matrices to simultaneously determine the concentration of chemical components throughout the binding process. This should be useful for establishing a protocol for using these analytical methodologies to monitor the binding reactions between the ligand and biomolecule.

■ ASSOCIATED CONTENT

Ⓢ Supporting Information

Additional figures and tables. This material is available free of charge via the Internet at http://pubs.acs.org.

■ AUTHOR INFORMATION

Corresponding Author

*(Y.N.) Phone: +86 791 83969500. Fax: +86 791 83969500. E-mail: ynni@ncu.edu.cn.

Funding

This research was supported by grants from the National Natural Science Foundation of China (NSFC-21065007) and the State Key Laboratory of Food Science and Technology of Nanchang University (SKLF-ZZA-201302, SKLF-ZZB-201303, and SKLF-KF-201004).

Notes

The authors declare no competing financial interest.

■ REFERENCES

(1) Bonnaud, M.; Weiss, J.; McClements, D. J. Interaction of a food-grade cationic surfactant (lauric arginate) with food-grade biopolymers (pectin, carrageenan, xanthan, alginate, dextran, and chitosan). *J. Agric. Food Chem.* **2010**, *58*, 9770–9777.

(2) Vanden Heuvel, J. P.; Kuslikis, B. I.; Van Rafelghem, M. J.; Peterson, R. E. Tissue distribution, metabolism, and elimination of perfluorooctanoic acid in male and female rats. *J. Biochem. Toxicol.* **1991**, *6*, 83–92.

(3) Kannan, K.; Yun, S. H.; Evans, T. J. Chlorinated, brominated, and perfluorinated contaminants in livers of polar bears from Alaska. *Environ. Sci. Technol.* **2005**, *39*, 9057–9063.

(4) Carter, D. C.; Ho, J. X. Structure of serum albumin. *Adv. Protein Chem.* **1994**, *45*, 153–203.

(5) Jones, M. N.; Brass, A. In *Food Polymers, Gels and Colloids*; Dickenson, E., Ed.; Royal Society of Chemistry: Cambridge, UK, 1991; pp 65–80.

(6) McClements, D. J. *Food Emulsions: Principles, Practice and Techniques*, 2nd ed.; CRC Press: Boca Raton, FL, 2005.

(7) Sharma, A.; Agarwal, P. K.; Deep, S. Characterization of different conformations of bovine serum albumin and their propensity to aggregate in the presence of *N*-cetyl-*N*,*N*,*N*-trimethyl ammonium bromide. *J. Colloid Interface Sci.* **2010**, *343*, 454–462.

(8) Singh, R. B.; Mahanta, S.; Guchhait, N. Destructive and protective action of sodium dodecyl sulphate micells on the native conformation of bovine serum albumin: a study by extrinsic fluorescence probe 1-hydroxy-2-naphthaldehyde. *Chem. Phys. Lett.* **2008**, *463*, 183–188.

(9) Qu, C. H.; Li, X. L.; Zhang, L.; Xi, C. U.; Wang, G. M.; Li, N. B.; Luo, H. Q. Simultaneous determination of cimaterol, salbutamol, terbutaline and ractopamine in feed by SPE coupled to UPLC. *Chromatographia* **2011**, *73*, 243–249.

(10) Shishani, E.; Chai, S. C.; Jamokha, S.; Aznar, G.; Hoffman, M. K. Determination of ractopamine in animal tissues by liquid chromatography-fluorescence and liquid chromatography/tandem mass spectrometry. *Anal. Chim. Acta* **2003**, *483*, 137–145.

(11) Wang, L. Q.; Zeng, Z. L.; Su, Y. J.; Zhang, G. K.; Zhong, X. L.; Liang, Z. P.; He, L. M. Matrix effects in analysis of β-agonists with LC-MS/MS: influence of analyte concentration, sample source, and SPE type. *J. Agric. Food Chem.* **2012**, *60*, 6359–6363.

(12) Ni, Y. N.; Zhang, Q. L.; Kokot, S. Analysis of the interactions of mixtures of two β-agonist steroids with bovine serum albumin: a fluorescence spectroscopy and chemometrics investigation. *Analyst* **2010**, *135*, 2059–2068.

(13) Zhang, Q. L.; Ni, Y. N.; Kokot, S. Molecular spectroscopic studies on the interaction between ractopamine and bovine serum albumin. *J. Pharm. Biomed. Anal.* **2010**, *52*, 280−288.
(14) Feroz, S. R.; Mohamad, S. B.; Bujang, N.; Malek, S. N. K.; Tayyab, S. Multispectroscopic and molecular modeling approach to investigate the interaction of flavokawain B with human serum albumin. *J. Agric. Food Chem.* **2012**, *60*, 5899−5908.
(15) Yang, J. H.; Zhao, J.; Xiao, J.; Xiao, H.; Zhang, D. M.; Li, G. X. Study of hemoglobin and human serum albumin glycation with electrochemical techniques. *Electroanalysis* **2011**, *23*, 463−468.
(16) Zhao, J.; Zheng, X. F.; Xing, W.; Huang, J. Y.; Li, G. X. Electrochemical studies of camptothecin and its interaction with human serum albumin. *Int. J. Mol. Sci.* **2007**, *8*, 42−50.
(17) Workman, J.; Koch, M.; Veltkamp, D. Process analytical chemistry. *Anal. Chem.* **2007**, *79*, 4345−4364.
(18) Peter, T. *All about Albumin: Biochemistry Genetics and Medical Applications*; Academic Press: San Diego, CA, 1996; pp 9−75.
(19) De Juan, A.; Tauler, R. Chemometrics applied to unravel multicomponent processes and mixtures. Revisiting latest trends in multivariate resolution. *Anal. Chim. Acta* **2003**, *500*, 195−210.
(20) Vives, M.; Gargallo, R.; Tauler, R. Multivariate extension of the continuous variations and mole-ratio methods for the study of the interaction of intercalators with polynucleotides. *Anal. Chim. Acta* **2000**, *424*, 105−114.
(21) Jaumot, J.; Gargallo, R.; de Juan, A.; Tauler, R. A graphical user-friendly interface for MCR-ALS: a new tool for multivariate curve resolution in MATLAB. *Chemom. Intell. Lab. Syst.* **2005**, *76*, 101−110.
(22) Gampp, H.; Maeder, M.; Meyer, C. J.; Zuberbühler, A. D. Calculation of equilibrium constants from multiwavelength spectroscopic data − III. Model-free analysis of spectrophotometric and ESR titrations. *Talanta* **1985**, *32*, 1133−1139.
(23) Abdollahi, H.; Mahdavi, V. Tautomerization equilibria in aqueous micellar solutions: a spectrophotometric and factor-analytical study. *Langmuir* **2007**, *23*, 2362−2368.
(24) Perez, I. S.; Culzoni, M. J.; Siano, G. G.; Gil Garcia, M. D.; Goicoechea, H. C. Detection of unintended stress effects based on a metabonomic study in tomato fruits after treatment with carbofuran pesticide. Capabilities of MCR-ALS applied to LC-MS three-way data arrays. *Anal. Chem.* **2009**, *81*, 8335−8346.
(25) Windig, W.; Guilment, J. Interactive self-modeling mixture analysis. *Anal. Chem.* **1991**, *63*, 1425−1432.
(26) Azzouz, T.; Tauler, R. Application of multivariate curve resolution alternating least squares (MCR-ALS) to the quantitative analysis of pharmaceutical and agricultural samples. *Talanta* **2008**, *74*, 1201−1210.
(27) Ni, Y. N.; Su, S. J.; Kokot, S. Small molecule-biopolymer interactions: ultraviolet-visible and fluorescence spectroscopy and chemometrics. *Anal. Chim. Acta* **2008**, *628*, 49−56.
(28) Leugans, S.; Ross, R. T. Multi models: application in spectroscopy. *Stat. Sci.* **1992**, *7*, 289−319.
(29) Escandar, G. M.; Faber, N. K. M.; Goicoechea, H. C.; de Ia Pena, A. M.; Olivieri, A. C.; Poppi, R. J. Second- and third-order multivariate calibration: data, algorithms and applications. *TrAC, Trends Anal. Chem.* **2007**, *26*, 752−765.
(30) Gil, D. B.; de la Pena, A. M.; Arancibia, J. A.; Escandar, G. M.; Olivieri, A. C. Second-order advantage achieved by unfolded-partial least-squares/residual bilinearization modeling of excitation-emission fluorescence data presenting inner filter effects. *Anal. Chem.* **2006**, *78*, 8051−8058.
(31) Ohno, T.; Amirbahman, A.; Bro, R. Parallel factor analysis of excitation-emission matrix fluorescence spectra of water soluble soil organic matter as basic for the determination of conditional metal binding parameters. *Environ. Sci. Technol.* **2008**, *42*, 186−192.
(32) Bro, R. PRAFAC: tutorial and applications. *Chemom. Intell. Lab. Syst.* **1997**, *38*, 149−171.
(33) Harshman, R. A. *Foundations of the PARAFAC Procedure: Models and Conditions for an "Explanatory" Multi-Model Factor Analysis*; UCLA Working Papers in Phonetics; University of California: Los Angeles, CA, 1970; Vol. 16, pp 1−84.
(34) Andersen, C. M.; Bro, R. Practical aspects of PARAFAC modelling of fluorescence excitation-emission data. *J. Chemom.* **2003**, *17*, 200−215.
(35) Bro, R. Review on multiway analysis in chemistry − 2000−2005. *Crit. Rev. Anal. Chem.* **2006**, *36*, 279−293.
(36) Maiti, T. K.; Ghosh, K. S.; Samanta, A.; Dasgupta, S. The interaction of silibinin with human serum albumin: a spectroscopic investigation. *J. Photochem. Photobiol. A: Chem.* **2008**, *194*, 297−307.
(37) Li, J. H.; Ren, C. L.; Zhang, Y. H.; Liu, X. Y.; Yao, X. J.; Hu, Z. D. Spectroscopic studies on binding of puerarin to human serum albumin. *J. Mol. Struct.* **2008**, *885*, 64−69.
(38) Lakowicz, J. R. *Principles of Fluorescence Spectroscopy*, 2nd ed.; Plenum Press: New York, 1999; pp 237−265.
(39) Marty, A.; Boiret, M.; Deumie, M. How to illustrate ligand-protein binding in class experiment: an elementary fluorescent assay. *J. Chem. Educ.* **1986**, *63*, 365−366.
(40) Gentili, P. L.; Ortica, F.; Favaro, G. Static and dynamic interaction of a naturally occurring photochromic molecule with bovine serum albumin studies by UV-visible absorption and fluorescence spectroscopy. *J. Phys. Chem. B* **2008**, *112*, 16793−16801.
(41) Dominguez-Vidal, A.; Saena-Navajas, M. P.; Ayora-Canada, M. J.; Lendl, B. Detection of albumin unfolding preceding proteolysis using Fourier transform infrared spectroscopy and chemometric data. *Anal. Chem.* **2006**, *78*, 3257−3264.
(42) Kelley, D.; McClements, D. J. Interactions of bovine serum albumin with ionic surfactants in aqueous solutions. *Food Hydrocolloids* **2003**, *17*, 73−85.
(43) Zhang, G. W.; Que, Q. M.; Pan, J. H.; Guo, J. B. Study of the interaction between icariin and human serum albumin by fluorescence spectroscopy. *J. Mol. Struct.* **2008**, *881*, 132−138.
(44) Sudlow, G.; Birkett, D. J.; Wade, D. N. Further characterization of specific drug binding sites on human serum albumin. *Mol. Pharmacol.* **1976**, *12*, 1052−1061.
(45) He, X. M.; Carter, D. C. Atomic structure and chemistry of human serum albumin. *Nature* **1992**, *358*, 209−215.
(46) Zhang, Y. Z.; Zhou, B.; Zhang, X. P.; Huang, P.; Li, C. H.; Liu, Y. Interaction of malachite green with bovine serum albumin: determination of the binding mechanism and binding site by spectroscopic methods. *J. Hazard. Mater.* **2009**, *163*, 1345−1352.
(47) Dufour, C.; Dangles, O. Flavonoid−serum albumin complexation: determination of binding constants and binding sites by fluorescence spectroscopy. *Biochim. Biophys. Acta* **2005**, *1721*, 164−173.